JOURNAL OF AIRCRAFT
Vol. 42, No. 1, January–February 2005

Analysis of Proprotor Whirl Flutter: Review and Update

Donald L. Kunz*
U.S. Air Force Institute of Technology, Wright–Patterson Air Force Base, Ohio 45433-7765

Whirl flutter instabilities have been a matter of concern for propeller-driven aircraft, aircraft having tilting proprotors, and helicopters ever since two Lockheed Electras crashed more than 40 years ago. A significant body of literature exists, which details the analyses used to predict whirl flutter and the experiments that have validated the analyses. The factors that contribute to whirl flutter are reviewed, and with use of simple analysis methods, their effect on stability are demonstrated. Whereas previous efforts in the literature have tended to concentrate exclusively on propellers, proprotors, or helicopter rotors, a unified treatment of all three configurations is presented.

Nomenclature

a	=	lift curve slope
b	=	number of blades
C_T	=	proprotor thrust coefficient
d	=	rotor undersling
H	=	rotor H force
h	=	rotor shaft length
I_b	=	blade moment of inertia, kg · m^2
I_{xx}, I_{yy}, I_{xy}	=	nacelle moments of inertia
M_b	=	blade mass
M_X	=	rotor lateral moment
M_Y	=	rotor longitudinal moment
R	=	proprotor radius, m
S_b	=	blade first moment of inertia
T	=	rotor thrust
Y	=	rotor Y force
β_c, β_s	=	rotor cyclic flapping degrees of freedom
β_{pc}	=	blade precone angle
β_x, β_y	=	rotor gimbal degrees of freedom
γ	=	Lock number
θ_0	=	blade root pitch angle
θ_{twist}	=	blade rate of twist
σ	=	rotor solidity
Φ_Y	=	nacelle tilt angle
ϕ	=	inflow angle
ϕ_x, ϕ_y	=	nacelle degrees of freedom
Ω	=	rotor speed
Ω_0	=	normal rotor speed, rad/s
ω_β	=	blade flapping frequency
ω_x, ω_y	=	nacelle natural frequencies

Introduction

ON 29 September 1959, a Lockheed L-188C Electra suffered the first documented occurrence of proprotor whirl flutter, which resulted in the loss of the aircraft and all persons aboard. The probable cause of the accident was listed as "Structural failure of the left wing resulting from forces generated by undampened propeller whirl mode."[1] A second occurrence on 17 March 1960 met with the same result. Again, the probable cause was listed as, "In-flight separation of the right wing because of flutter induced by oscillation of the outboard nacelles."[2] In this case, "Reduced stiffness of the structure" was listed as a contributing factor. As a result of these tragic accidents, proprotor whirl flutter became a matter of concern for all propeller-driven aircraft, as well as tilting proprotor aircraft and helicopters.

A search of the literature shows that before 1960, proprotor whirl flutter had not been investigated analytically or experimentally and was only barely recognized as potential problem. In 1938, Taylor and Browne[1] suggested that the "low-frequency reverse-rotating precession" mode may become unstable under certain conditions. However, they were not able to produce this instability using existing configurations of aircraft powerplants. Scanlan and Truman[2] investigated a propeller configuration that probably would have produced a dynamic instability had aerodynamic forces been included in their analysis, 12 years later.

The impetus for in-depth investigation of whirl flutter was, of course, the loss of the two aircraft due to catastrophic instabilities. NASA Langley Research Center was the focal point for both the analytical and experimental aspects of the research. In 1962, Houbolt and Reed[3] published the first paper that described the whirl flutter instability, backed by analysis using a mathematical model of a propeller. The model presented in that paper was based on a NASA report authored by Reed and Bland,[4] in which the analytical model was developed. The principal findings in Ref. 3 were that whirl flutter is strongly dependent on the nacelle pivot location, stiffness, and damping. These findings confirmed the probable cause and contributing factor that were identified for both Electra crashes. After several more years of analytical and experimental investigations of whirl flutter, Reed[5] summarized the state of the art. In addition to previous findings, it was shown that flapping blades introduce the possibility of forward whirl instabilities, in addition to the backward whirl instability exhibited by rigid propellers. Also, wing flexibility was shown to be a stabilizing factor in most cases.

By the mid-1960s, jet engines were replacing turboprop engines, and proprotor whirl flutter could have easily become a footnote to the history of aviation. However, recent developments in advanced turboprop aircraft, whose blades have nontraditional planforms, have contributed to a renewed interest in propeller whirl flutter.[6] In addition, wind turbines[7] and high-endurance aircraft[8] have exhibited instances of whirl flutter instabilities.

Another reason for continued interest in whirl flutter was due to new configurations of vertical takeoff and landing (VTOL) aircraft, that were being investigated as replacements for fixed-wing aircraft and helicopters for short-haul operations. Two of the more promising configurations, tilt-wing and tilt-rotor aircraft, employed proprotors to generate thrust. The rotors on the tilt-wing aircraft had a somewhat larger diameter than conventional turboprop propellers, and the rotor nacelles were rigidly attached to the pivoting wing. The diameter of the rotors on the tilt-rotor was larger than those on the tilt-wing, but small compared to helicopter rotors. Also the nacelles pivoted at the end of the wing. The tilt-rotor was found to

Presented as Paper 2002-1602 at the AIAA/ASME/ASCE/AHS/ASC 43rd Structures, Structural Dynamics and Materials Conference, Denver, CO, 22 April 2003; received 3 September 2003; revision received 7 April 2004; accepted for publication 7 April 2004. This material is declared a work of the U.S. Government and is not subject to copyright protection in the United States. Copies of this paper may be made for personal or internal use, on condition that the copier pay the $10.00 per-copy fee to the Copyright Clearance Center, Inc., 222 Rosewood Drive, Danvers, MA 01923; include the code 0021-8669/05 $10.00 in correspondence with the CCC.

*Associate Professor, Department of Aeronautics and Astronautics, 2950 Hobson Way. Associate Fellow AIAA.

be particularly susceptible to whirl flutter because of its larger rotor and the additional flexibility introduced by the tilting mechanism.

A number of analytical investigations were performed, to develop a better understanding of whirl flutter on tilt-rotor aircraft. Among the first of these investigations was Hall's study[9] of a 1962 whirl flutter incident during an XV-3 wind-tunnel test. One of the principal contributions of Hall's work was in identifying the influence of pitch–flap coupling on whirl stability. In a paper published in 1967, Young and Lytwyn[10] showed analytically that the fundamental blade flapping frequency could be defined to obtain an optimum rotor design with respect to whirl flutter. However, this criterion does not account for blade flapping and oscillatory blade loads during maneuvers,[11] which can also be important design considerations. Another study,[12] using a combination of analysis and testing, investigated the effects of pylon stiffness, swashplate–pylon coupling, pitch–flap coupling, blade flapping, and wing flexibility on whirl stability. Later, Kaza[13] investigated the effect of blade coning on whirl flutter stability. Recent investigations of whirl flutter have emphasized improved prediction methods[14] and improvements in tilt-rotor designs,[15] particularly for advanced geometries.[16]

Whereas whirl flutter had been observed on both propeller-driven and VTOL aircraft flying at high forward speeds, the instability had not been a concern for helicopters, which fly at relatively low forward speeds. However, a forward whirl flutter[17] was predicted and observed during the phase one development of the YAH-64 advanced attack helicopter (Apache). The cause of the instability was the coupling between the blade pitch angle and bending of the rotor mast. During the development of the AH-64D Longbow Apache, the instability reappeared[18] due to the presence of a mast-mounted assembly located above the plane of the rotor.

Whirl Flutter Model

Figure 1 is a schematic of the model used in this paper. Figure 1a shows the rotor as viewed looking down the Z axis, whereas Fig. 1b shows the rotor as viewed from the side. The X axis points up when the tilt angle Φ_Y is 0 deg and aft when the tilt angle is 90 deg. Point O is the location where the nacelle pivots in pitch and yaw, whereas G designates the gimbal joint and H is the flapping hinge location. The freestream air, $\mu\Omega R$, moves from right to left.

The quasi-steady aerodynamic forces used to define the aerodynamic damping and stiffness are derived using a typical blade cross-section, as shown in Fig. 2. The incremental lift and drag on

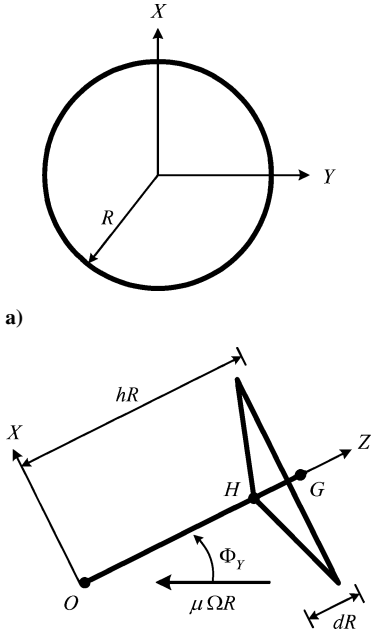

Fig. 1 Proprotor schematic.

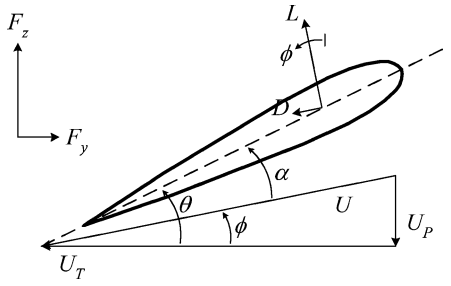

Fig. 2 Blade cross section schematic.

the cross section may be written as

$$\frac{\mathrm{d}L}{\mathrm{d}r} = \frac{\gamma}{bR^2}(\theta - \phi)\left(U_T^2 + U_P^2\right) \tag{1}$$

$$\frac{\mathrm{d}D}{\mathrm{d}r} = \frac{\gamma}{bR^2}\left(U_T^2 + U_P^2\right)\delta \tag{2}$$

where $\theta = \theta_0 + r\theta_{\text{twist}}$. The incremental forces in the x direction and y direction are then

$$\frac{\mathrm{d}F_y}{\mathrm{d}r} = -\frac{\gamma}{bR^2}\Omega^2[U_p U(\theta_0 - \phi) + U_T U\delta] \tag{3}$$

$$\frac{\mathrm{d}F_z}{\mathrm{d}r} = \frac{\gamma}{bR^2}\Omega^2[U_T U(\theta - \phi) - U_P U\delta] \tag{4}$$

The velocities U_T and U_P, as well as U and the inflow angle ϕ, may be separated into periodic and perturbation components,

$$U_T = u_T + \delta u_T \tag{5}$$

$$U_p = u_p + \delta u_P \tag{6}$$

$$U = u + \delta u = \sqrt{u_T^2 + u_P^2} + (u_T\delta u_T + u_p\delta u_p)/u \tag{7}$$

$$\phi = \phi_0 + \delta\phi = \tan^{-1}(u_p/u_T) + (u_T\delta u_P - u_P\delta u_T)/u \tag{8}$$

where

$$u_T = \bar{r}\cos\beta_{\text{pc}} + \mu\sin\Phi_Y\sin\psi_k \tag{9}$$

$$u_p = (\mu\cos\Phi_Y + \phi_i)\cos\beta_{\text{pc}} + \mu\sin\Phi_Y\sin\beta_{\text{pc}}\cos\psi_k \tag{10}$$

The quantities δu_T and δu_P contain terms that eventually form the coefficients of the aerodynamic damping and stiffness matrices.

The rotor forces and moments are obtained by integrating over the radius of each blade and then summing over all of the blades. For configurations where Φ_Y and μ are both nonzero, the coefficients of the aerodynamic damping and stiffness matrices are periodic. In those cases, the rotor forces and moments are subsequently averaged over the rotor azimuth so that the matrix coefficients become constants.[19] Equations (11–15) define the rotor forces and moments:

$$T = \sum_{k=1}^{b}\int_0^1 \left(\frac{\mathrm{d}F_z}{\mathrm{d}r}\right)\mathrm{d}r \tag{11}$$

$$H = \sum_{k=1}^{b}\int_0^1 \left(\frac{\mathrm{d}F_y}{\mathrm{d}r}\right)\mathrm{d}r\sin\psi_k \tag{12}$$

$$Y = \sum_{k=1}^{b}\int_0^1 \left(\frac{\mathrm{d}F_y}{\mathrm{d}r}\right)\mathrm{d}r\cos\psi_k \tag{13}$$

$$M_X = \sum_{k=1}^{b}\int_0^1 r\left(\frac{\mathrm{d}F_z}{\mathrm{d}r}\right)\mathrm{d}r\sin\psi_k \tag{14}$$

$$M_Y = -\sum_{k=1}^{b}\int_0^1 r\left(\frac{\mathrm{d}F_z}{\mathrm{d}r}\right)\mathrm{d}r\cos\psi_k \tag{15}$$

Propeller

The minimum mathematical model required to demonstrate classical whirl flutter consists of a rigid propeller with nacelle pitch and yaw degrees of freedom. The structural terms in the equations of motion for this model can be easily derived from either Hamilton's principle or Lagrange's equations and are

$$\left[I_{xx} + \tfrac{1}{2}(3 - \cos 2\beta_{\text{pc}}) + 4S_b(h-d)\sin\beta_{\text{pc}} + 2M_b(h-d)^2\right]\phi_x'' - (I_{xy})\phi_y'' + \left(2\Omega\cos^2\beta_{\text{pc}}\right)\phi_y' + \left(\omega_x^2 I_{xx}\right)\phi_x = M_{\phi_x} \tag{16}$$

$$-(I_{xy})\phi_x'' + \left[I_{yy} + \tfrac{1}{2}(3 - \cos 2\beta_{\text{pc}}) + 4S_b(h-d)\sin\beta_{\text{pc}} + 2M_b(h-d)^2\right]\phi_y'' - \left(2\Omega\cos^2\beta_{\text{pc}}\right)\phi_x' + \left(\omega_y^2 I_{yy}\right)\phi_y = M_{\phi_y} \tag{17}$$

The aerodynamic moments on the right-hand side of the equations are obtained from the forces and moments at the rotor hub,

$$M_{\phi_x} = M_X - hY \tag{18}$$

$$M_{\phi_y} = M_Y - hH \tag{19}$$

This simple, two-degree-of-freedom system can be readily used to demonstrate the effect of each of the system parameters on whirl flutter stability.

Gimballed Rotor

Present day tiltrotor aircraft designs employ a gimballed rotor system, usually with a small amount of undersling. The model shown in Fig. 1 is fully capable of representing the behavior of such a model. Like the classical model, the structural terms for the gimbal model are easily derived from Lagrange's equations or Hamilton's principle. The aerodynamic terms are also derived in the manner described earlier, where the only substantial modifications are in δu_T and δu_P. The modifications result from the addition of the two gimbal degrees of freedom. On the right-hand side of the equations of motion, the aerodynamic moments are defined as

$$M_{\phi_x} = M_X - (h-d)Y \tag{20}$$

$$M_{\phi_y} = M_Y - (h-d)H \tag{21}$$

$$M_{\beta_x} = M_X + dY \tag{22}$$

$$M_{\beta_y} = M_Y + dH \tag{23}$$

Helicopter Rotors

Most helicopters have a rotor system in which the rotor blades are allowed to flap. The rotor system shown in Fig. 1 models the blades using a central flapping hinge and a flapping restraint spring. The aerodynamic moments about the nacelle pivot and the rotor hub are

$$M_{\phi_x} = M_X - hY \tag{24}$$

$$M_{\phi_y} = M_Y - hH \tag{25}$$

$$M_{\beta_c} = -M_Y \tag{26}$$

$$M_{\beta_s} = M_X \tag{27}$$

Stability Calculation

The stability calculations shown in this paper were performed using a program written with OCTAVE,[20] a freely available language that is mostly compatible with MATLAB®. After the configuration parameters were defined, the trim state of the blade root pitch angle and the induced flow was calculated, based mainly on the thrust coefficient and advance ratio.[21]

For each of the three configurations described earlier, a set of nominal parameters is defined (Table 1). Unless otherwise noted, all of the calculations were performed using these parameters.

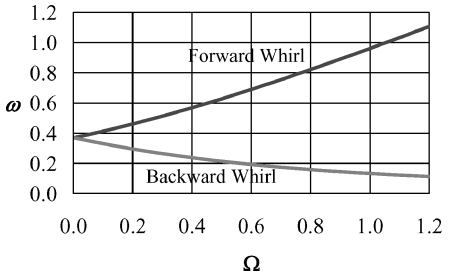

Fig. 3 Propeller whirl frequencies vs rotor speed, $C_T = 0$.

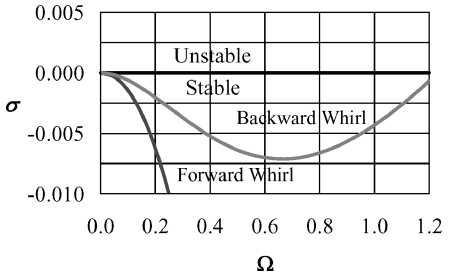

Fig. 4 Propeller whirl damping vs rotor speed, $C_T = 0$.

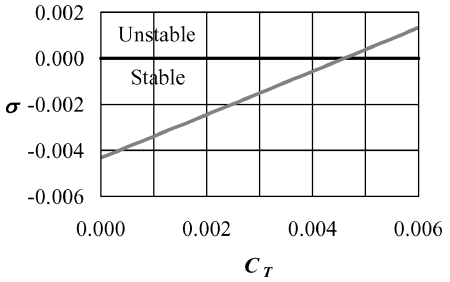

Fig. 5 Propeller backward whirl damping vs thrust coefficient.

Propeller Whirl Stability

The physical phenomenon of whirl flutter is easily understandable for the case of rigid propellers, like those used by conventional, fixed-wing, propeller-driven aircraft. For the classic propeller problem, the simple mathematical model described earlier is sufficient to illustrate the salient characteristics of propeller whirl flutter. Figure 3 shows the frequency characteristics of the propeller as a function of rotor speed. As shown in Ref. 5, the higher-frequency mode is the forward whirl mode, and the lower-frequency mode is the backward whirl mode.

Figure 4 shows that the damping in the backward whirl mode initially increases with rotor speed, but then decreases to the point where it eventually becomes unstable (beyond the range of Fig. 4).

Most of the analytical results shown in Ref. 5 and Figs. 3 and 4 show the frequency and damping properties of a propeller that is windmilling, $C_T = 0$. Figure 5 shows that, as the amount of thrust produced by the propeller increases, the propeller damping decreases. Predictably, a comparison of Figs. 4 and 6 shows that the propeller that is producing thrust has poorer stability characteristics than the windmilling propeller. The frequency characteristics are nearly identical, however.

Propeller whirl stability is known to be highly sensitive to advance ratio, as shown in Fig. 7. On some aircraft, particularly tiltrotors such as the XV-15 and V-22, the whirl stability boundary is the determining factor for the aircraft top speed in level flight.

As shown in Ref. 5, the natural frequencies of the nacelle pivot joint also play a significant role in the whirl stability of a propeller. Figure 8 shows the backward whirl mode frequencies vs the yaw natural frequency for three values of the pitch natural frequency. It can be clearly seen from Fig. 8 that all three cases are divergent (zero frequency) when the yaw natural frequency is small (low stiffness).

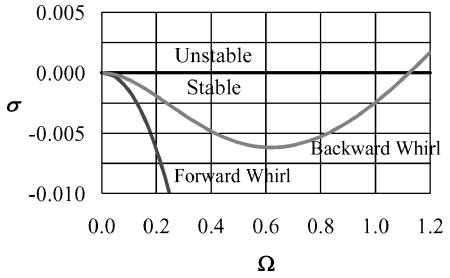

Fig. 6 Propeller whirl damping vs rotor speed, $C_T = 0.002$.

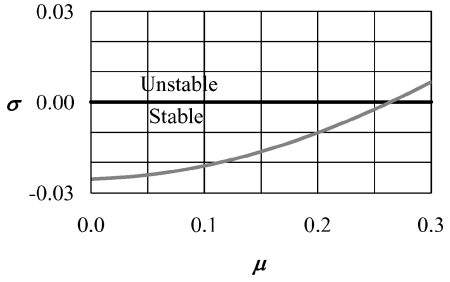

Fig. 7 Propeller backward whirl damping vs advance ratio.

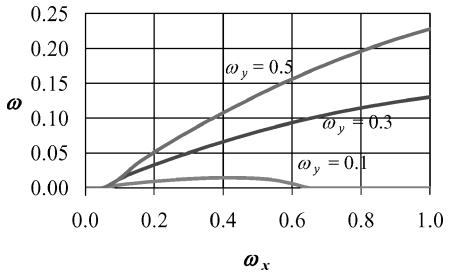

Fig. 8 Propeller backward whirl frequency vs nacelle frequency.

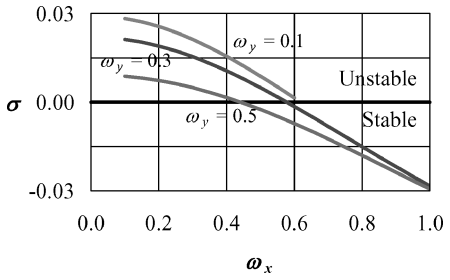

Fig. 9 Propeller backward whirl damping vs nacelle frequency.

The case of $\omega_y = 0.1$ is also divergent at high values of yaw natural frequency. The effect of the nacelle natural frequencies on whirl stability is shown in Fig. 9. Clearly, excessive flexibility in the nacelle pivot joint has an adverse effect on whirl stability.

In addition to the configuration parameters already discussed, parametric variations of the length of the rotor shaft, the blade rate of twist, and the blade precone were performed. Increasing the length of the rotor shaft is stabilizing. This result may at first appear to be in conflict with earlier observations because increasing the length of the rotor shaft increases the total inertia and decreases the nacelle natural frequency. However, by the increase of the total inertia, the energy required to drive the instability is increased. Increases in rate of twist and precone are also stabilizing, but are weak effects.

Aircraft such as the LTV-Hiller-Ryan XC-142 and the Canadair CL-84 used propeller thrust for lift at low advance ratios by tilting their wings from the horizontal position to the vertical position. It should be obvious that, as the tilt angle increases, the advance ratio must decrease because more of the propeller thrust must be used for

Table 1 Nominal configuration parameters

Parameter	Propeller	Tiltrotor	Helicopter
I_{xx}	1.325	1.325	1.325
I_{yy}	1.325	1.325	1.325
ω_x	0.5	1.2	2.2
ω_y	0.5	1.2	2.2
h	0.25	0.35	0.25
d	n/a	0	n/a
Ω	1.0	1.0	1.0
b	3	3	4
M_b	0.75	0.75	0.75
S_b	0.375	0.375	0.375
ω_β	n/a	n/a	0.5
β_{pc}, deg	0	0	0
C_T	0.002	0	0.005
μ	0.25	1.2	0
Φ_Y, deg	0	0	90
γ	4	4	6
σ	0.2	0.1	0.1
δ	0.01	0.01	0.01
θ_{twist}, deg	−75	−45	−10

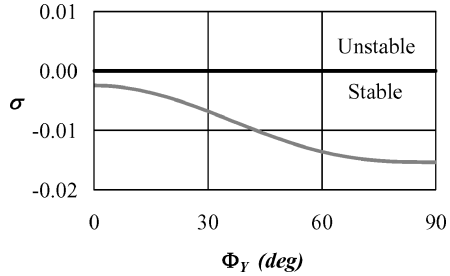

Fig. 10 Propeller damping vs nacelle tilt.

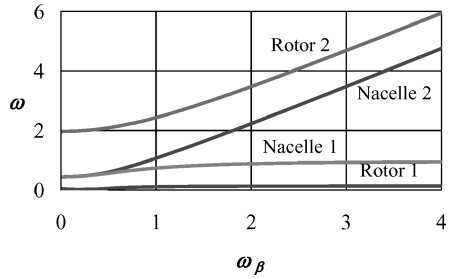

Fig. 11 Propeller frequencies vs nonrotating flap frequency.

maintaining lift. As shown in Fig. 10, tilt angle has a strong stabilizing effect on the whirl mode. The influence of the nacelle tilt angle can be seen to be a significant factor in forthcoming discussions of tiltrotor aircraft and helicopters. Like tiltwing aircraft, the tilt angle of a tiltrotor aircraft is 90 deg in hover, whereas the tilt angle is close to 90 deg for all helicopter flight conditions.

Although blade flexibility is not a significant factor for most propellers, in Ref. 5 its effect is discussed by introducing a flapping hinge that is offset from the hub center. A brief discussion of blade flexibility at this point does provide a good starting point for the discussions of tiltrotor aircraft and helicopters to follow. In this paper, blade flexibility is incorporated into the model by introducing a central flapping hinge that includes a flapping spring. A relationship between hinge offset and flapping spring stiffness can be defined based on equating the rotating flap frequencies,

$$\omega_\beta^2 = \tfrac{3}{2}e \tag{28}$$

When the propeller configuration parameters defined in Table 1 were used, blade flapping degrees of freedom were introduced into the model. Figure 11 shows the natural frequencies of the resulting system as a function of the blade nonrotating flap frequency. The modes with the highest and lowest frequencies start out as the

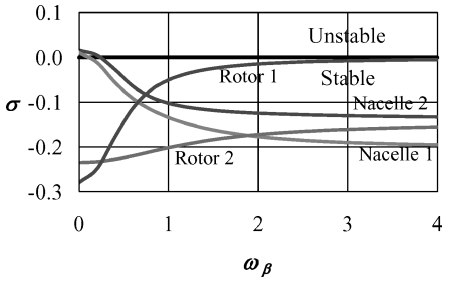

Fig. 12 Propeller damping vs nonrotating flap frequency.

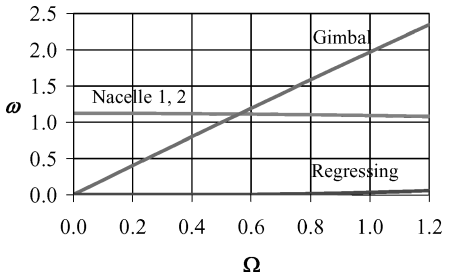

Fig. 13 Gimbaled rotor frequencies vs rotor speed.

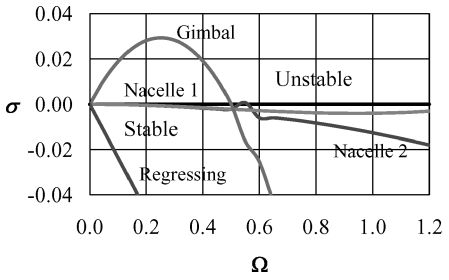

Fig. 14 Gimbaled rotor damping vs rotor speed.

progressing and regressing cyclic flapping modes, respectively. For a nonrotating flap frequency of zero, flapping motion is equivalent to gimbal motion with no undersling. The two intermediate modes start out as the nacelle modes.

As the flap frequency increases, the rigid propeller condition is approached, and the two lower-frequency modes become the forward and backward whirl modes As seen in Fig. 12, which shows the modal damping as a function of the flap frequency, the regressing flap mode becomes the backward whirl mode as the flap spring becomes very stiff. The mode that starts out as the more heavily damped of the two nacelle modes becomes the forward whirl mode.

Tiltrotor Whirl Stability

The dominant design in use today for tiltrotor aircraft is the gimbaled rotor, with a small amount of undersling. Table 1 contains a listing of the nominal configuration parameters used for demonstrating the characteristics of whirl flutter in tiltrotor aircraft.

Figure 13 shows the natural frequencies of the gimbal rotor as a function of rotor speed. As expected, the progressing gimbal mode frequency increases linearly with rotor speed, whereas the regressing mode frequency stays close to zero. The nacelle modes are nearly coincident and are relatively constant with rotor speed. Because of the scale, Fig. 13 does not show that one of the nacelle modes couples with the progressing flap mode in the vicinity where they cross. The coupling effect can be seen more clearly in Fig. 14, where both modes exhibit a small hump at the rotor speed where they cross. Note that the progressing flap mode is unstable until the rotor speed reaches a value of 0.5. As shown in Fig. 12, this instability can be eliminated by adding a small amount of stiffness to the gimbal joint.

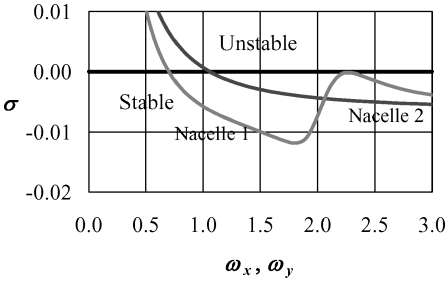

Fig. 15 Gimbaled rotor damping vs pivot frequency.

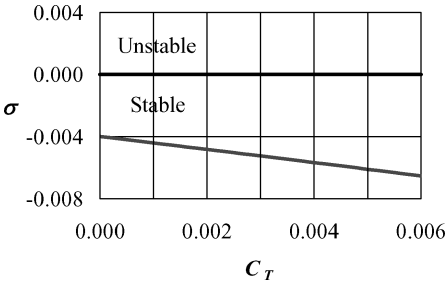

Fig. 16 Gimbaled rotor damping vs thrust coefficient.

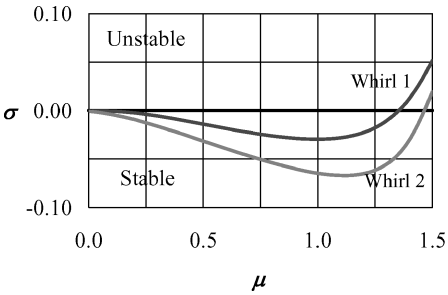

Fig. 17 Gimbaled rotor damping vs advance ratio.

Whereas increasing the stiffness (natural frequency) of the nacelle pivot generally improves the whirl stability characteristics of the gimbaled rotor, one must be careful in the vicinity where the progressing flap mode and the pivot frequency are nearly equal. As shown in Fig. 15, one of the nacelle modes becomes very lightly damped just after crossing the progressing flap mode.

As can be seen from Table 1, the nominal thrust coefficient for the gimbaled rotor is zero, whereas for the propeller it was nonzero. The reason for this difference is shown in Fig. 16. In the case of the gimbaled rotor, increasing thrust coefficient is stabilizing, and so the critical condition is a windmilling rotor.

As in the case of the propeller, the whirl instability is encountered when the advance ratio becomes sufficiently large. However, as shown in Fig. 17, the damping levels drop off much more rapidly than in the case of the propeller. Also, at a sufficiently high advance ratio, both whirl modes can be unstable.

To minimize the blade-bending moments at the root of the rotor blades, gimbaled rotors are often designed with a small amount of builtin precone. In this manner, at the design thrust condition, the precone and the coning angle are equal and the moment due to blade bending is a minimum. Figure 18 shows that a small amount of precone is stabilizing, but that too much is destabilizing.

If the rotor is designed with precone (or cones due to thrust), the rotor center of gravity moves to a position above the rotor hub. This increases the moment on the gimbal joint and to the rotor shaft. To negate the effect of the precone, gimbaled rotor are often designed with undersling, which positions the rotor hub below the gimbal joint (Fig. 1). The destabilizing effect of adding undersling to a rotor is shown in Fig. 19. To keep the rotor center of gravity at the

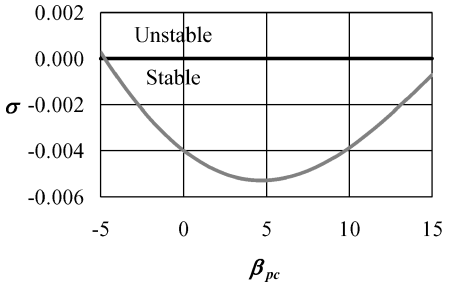

Fig. 18 Gimbaled rotor damping vs precone.

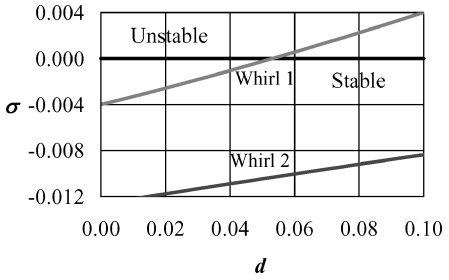

Fig. 19 Gimbaled rotor damping vs undersling.

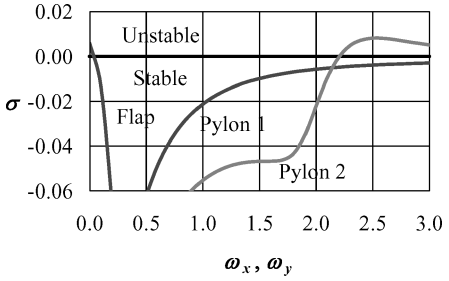

Fig. 20 Helicopter rotor damping vs pylon frequencies.

gimbal joint, the following relationship exists between undersling and precone:

$$d = \tfrac{1}{2} \sin \beta_{\text{pc}} \tag{29}$$

The implication from Eq. (29) is that, for every degree of precone, the rotor must be underslung 0.0087. Based on Figs. 18 and 19, the combination of precone and undersling is always slightly destabilizing.

Helicopter Whirl Stability

In the cases of propeller-driven aircraft, tiltwing aircraft, and tiltrotor aircraft, high-speed flight is attained with the proprotor in the horizontal position. As already shown, this orientation is the most critical condition for whirl flutter. Helicopter rotors, on the other hand, are always in a nearly vertical position, because they have no wings to provide auxiliary lift. In spite of this, helicopter rotors may also be susceptible to whirl flutter.[17,18]

In Refs. 17 and 18, the role is discussed of pitch/mast–bending coupling on whirl flutter as experienced on the AH-64A Apache helicopter. These studies concluded that flap coupling should be minimized to mitigate the onset of whirl flutter. In addition, the stiffness of the pylon support was also determined to be significant because it is the primary source of pitch/mast–bending coupling. Figure 20 shows how the pylon stiffness influences helicopter whirl flutter, in the absence of flap coupling. When the value of pylon frequencies are close to 2.0, there is evidence that one of the pylon modes couples with the progressing flap mode. As the pylon frequency continues to increase, an instability is observed. The curves in Fig. 21 have the interesting characteristic that the instability occurs when either pylon frequency exceeds a threshold frequency that is slightly greater

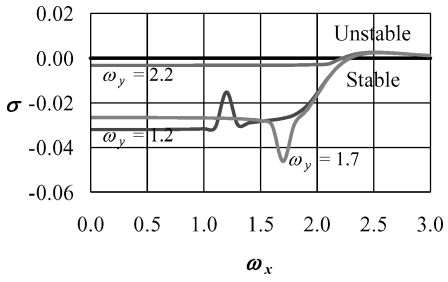

Fig. 21 Helicopter rotor damping vs pylon frequency variations.

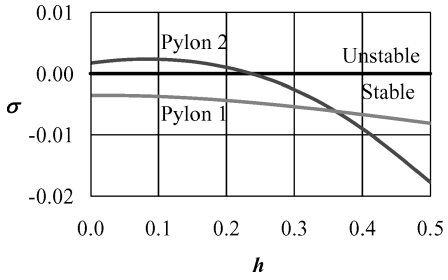

Fig. 22 Helicopter rotor damping vs mast height.

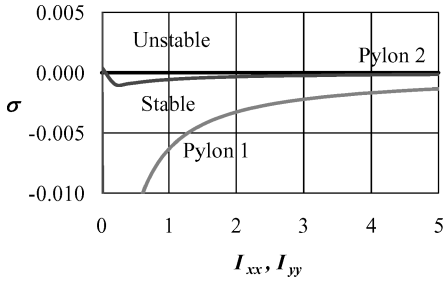

Fig. 23 Helicopter rotor damping vs pylon moments of inertia.

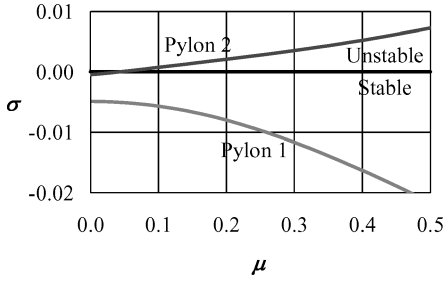

Fig. 24 Helicopter rotor damping vs advance ratio.

than 2.2. The effect of coupling with the progressing flap mode is also evident in Fig. 21.

During the development of the Apache, it became necessary to raise the rotor to reduce vibrations due to the rotor wake impinging on the fuselage. Figure 22 shows the stabilizing effect of raising the rotor.

In military applications, the tactical advantage of placing target acquisition and designation sensors and electronics above the rotor of helicopters has led to placing mast-mounted assemblies (MMAs) on helicopters like the AH-64D Longbow Apache, RAH-66 Comanche, and OH-58D Kiowa Warrior. The curves in Fig. 23 indicate that increasing the MMA mass or MMA height (which combine to increase the pylon moment of inertia) has a weakly destabilizing effect.

Figure 24 shows the destabilizing effect of advance ratio. It is evident from Fig. 24 that, if the stability margin is small in hover, a whirl stability problem is likely in high-speed forward flight. Similarly, Fig. 25 shows that thrust coefficient (in hover) has a weak,

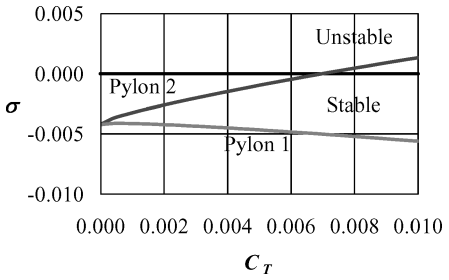

Fig. 25 Helicopter rotor damping vs thrust coefficient.

destabilizing effect. Under heavy load conditions, a helicopter with marginal stability may be subject to a whirl instability.

Conclusions

A review of the basic elements of whirl flutter analysis has been presented, and it includes propellers, tilting proprotors, and helicopters. Although the equations of motion are simplified, all of the degrees of freedom and system parameters required to demonstrate the characteristics of whirl stability are included for each configuration.

As one would expect, there are many similarities between the characteristics of propellers and gimbaled rotors, but the gimbal degrees of freedom do have a significant influence on the dynamics of the rotor system. The similarities between gimbaled rotors and flapping rotors are even greater because gimbal motion and cyclic flapping are equivalent under certain circumstances. However, the fact that helicopters never operate with a horizontal rotor orientation is a significant difference.

References

[1]Taylor, E. S., and Browne, K. A., "Vibration Isolation of Aircraft Power Plants," *Journal of the Aeronautical Sciences*, Vol. 6, No. 2, 1938, pp. 43–49.

[2]Scanlan, R. H., and Truman, J. C., "The Gyroscopic Effect of a Rigid Rotating Propeller on Engine and Wing Vibration Modes," *Journal of the Aeronautical Sciences*, Vol. 17, No. 10, 1950, pp. 653–659, 666.

[3]Houbolt, J. C., and Reed, W. H., III, "Propeller-Nacelle Whirl Flutter," *Journal of the Aerospace Sciences*, Vol. 29, No. 3, 1962, pp. 333–346.

[4]Reed, W. H., III, and Bland, S. R., "An Analytical Treatment of Aircraft Propeller Precession Instability," NASA TN D-659, Jan. 1961.

[5]Reed, W. H., III, "Propeller-Rotor Whirl Flutter: A State-of-the-Art Review," *Journal of Sound and Vibration*, Vol. 4, No. 3, 1966, pp. 526–544.

[6]Nitzsche, F., "Whirl-Flutter Suppression in Advanced Turboprops and Turbofans by Active Control Techniques," *Journal of Aircraft*, Vol. 31, No. 3, 1994, pp. 713–719.

[7]Janetzke, D. C., and Kaza, K. R. V., "Whirl Flutter Analysis of a Horizontal-Axis Wind Turbine with a Two-Bladed Teetering Rotor," *Solar Energy*, Vol. 31, No. 2, 1983, pp. 173–182.

[8]Singh, B., and Chopra, I., "Whirl Flutter Stability of Two-Bladed Proprotor/Pylon Systems in High Speed Flight," *Journal of the American Helicopter Society*, Vol. 48, No. 2, 2003, pp. 99–107.

[9]Hall, W. E., Jr., "Propeller-Rotor Stability at High Advance Ratios"' *Journal of the American Helicopter Society*, Vol. 11, No. 3, 1966, pp. 11–26.

[10]Young, M. I., and Lytwyn, R. T., "The Influence of Blade Flapping Restraint on the Dynamic Stability of Low Disk Loading Propeller-Rotors," *Journal of the American Helicopter Society*, Vol. 12, No. 4, 1967, pp. 11–26.

[11]Wernicke, K. G., and Gaffey, T. M., "Review and Discussion of 'The Influence of Blade Flapping Restraint on the Dynamic Stability of Low Disk Loading Propeller-Rotors,' " *Journal of the American Helicopter Society*, Vol. 12, No. 4, 1967, pp. 55–60.

[12]Edenborough, H. K., "Investigation of Tilt-Rotor VTOL Aircraft Rotor-Pylon Stability," *Journal of Aircraft*, Vol. 5, No. 6, 1968, pp. 97–105.

[13]Kaza, K. R. V., "Effect of Steady-State Coning Angle and Damping on Whirl Flutter Stability," *Journal of Aircraft*, Vol. 10, No. 11, 1973, pp. 664–669.

[14]Hathaway, E. L., and Gandhi, F. S., "Modeling Refinements in Simple Tiltrotor Whirl Flutter Analyses," *Journal of the American Helicopter Society*, Vol. 48, No. 3, 2003, pp. 186–198.

[15]Acree, C.W., Jr., Johnson, W., and Peyran, R. J., "Rotor Design Options for Improving Tiltrotor Whirl Flutter Stability Margins," *Journal of the American Helicopter Society*, Vol. 46, No. 2, 2001, pp. 87–95.

[16]Srinivas, V., Chopra, I., and Nixon, M. W., "Aeroelastic Analysis of Advanced Geometry Tiltrotor Aircraft," *Journal of the American Helicopter Society*, Vol. 43, No. 3, 1998, pp. 212–221.

[17]Silverthorn, L. J., "Whirl Mode Stability of the Main Rotor of the YAH-64 Advanced Attack Helicopter," *Proceedings of the 38th Annual Forum of the American Helicopter Society*, American Helicopter Society, Alexandria, VA, 1982, pp. 80–89.

[18]Kunz, D. L., "On the Effect of Pitch/Mast-Bending Coupling on Whirl-Mode Stability," *Proceedings of the 48th Annual Forum of the American Helicopter Society*, American Helicopter Society, Alexandria, VA, 1992, pp. 87–93.

[19]Johnson, W., "Analytical Modeling Requirements for Tilting Proprotor Aircraft Dynamics," NASA TN D-8013, July 1975.

[20]Eaton, J. W., "GNU Octave—A High-Level Interactive Language for Numerical Computations" [online], URL:http://www.octave.org/doc/octave_toc.html [cited 23 March 2004].

[21]Johnson, W., "Dynamics of Tilting Proprotor Aircraft in Cruise Flight," NASA TN D-7677, May 1974.